Journal of Molecular Structure, 298 (1993) 177–190
0022-2860/93/$06.00

PIDOTIMOD, a new immunostimulating dipeptide, studied by molecular mechanics, normal mode analysis and dynamics calculations[1]

Vincenzo Villani[a,*], Rachele Pucciariello[a], Tiziano Crimella[b], Riccardo Stradi[c]

[a]*Dipartimento di Chimica, Universita' della Basilicata, Via N. Sauro 85, 85100 Potenza, Italy*
[b]*Poli Industria Chimica S.p.A., 20089 Quinto de' Stampi, Rozzano (MI), Italy*
[c]*Facolta' di Farmacia, Universita' di Milano Viale Abruzzi, Milano, Italy*

(First received 8 December 1992; in final form 9 March 1993)

Abstract

A theoretical study of PIDOTIMOD, a new immunostimulating dipeptide, using a combination of molecular mechanics, normal mode analysis and dynamics methods, has been carried out. The results have been compared with the experimental ones obtained using NMR spectroscopy. Conformational calculations and NMR spectra identify two classes of conformers, trans and cis, around the peptide bond between the rings, with relative conformational populations of 0.55 and 0.45, respectively. The best agreement is obtained using a dielectric constant $\epsilon = 7$ in the calculations. The conformational features show that the path connecting the trans and the cis forms may involve the rotation of the bridged peptide bond alone. From a dynamic point of view the conformers appear rather rigid, and only the oxo-prolyl ring and the carboxyl group show significant rigid body-like motions. Interesting correlations occur in the fluctuations of the torsion angles.

Introduction

PIDOTIMOD (3-(5-oxo-L-prolyl)-L-thiazolidine-4-carboxylic acid), a synthetic dipeptide [1] (Fig. 1), has been shown to affect in a positive way some immune functions both in animals and in humans. It induces an increase in the expression of the Interleukin-2 (IL-2) T-lymphocyte receptor (functional activation) and could play an important role as an immunostimulating agent, improving immuno-defences [2,3].

In this paper, a theoretical study of PIDOTIMOD, using a combination of molecular mechanics, normal mode analysis and dynamics methods, is described. The results are compared with the experimental ones obtained using NMR spectroscopy. Using a systematic sampling procedure and molecular mechanics energy minimization, we have performed an exhaustive conformational analysis.

Normal mode analysis was used to carry out a general vibrational analysis with a molecular potential approach. The vibrational frequencies and the amplitudes of the normal modes were determined. The harmonic contribution to the thermodynamic variables of state was calculated.

Normal mode dynamics were used to describe slow collective molecular motions and conformational rearrangements. The behaviour of the structural parameters as a function of time, the time-averaged properties of the motion, the

*Corresponding author.

[1]Cartesian coordinates in pdb (Brookehaven protein data base) format, and vibrational normal mode frequencies and amplitudes for all the conformers are available on magnetic tape from the authors.

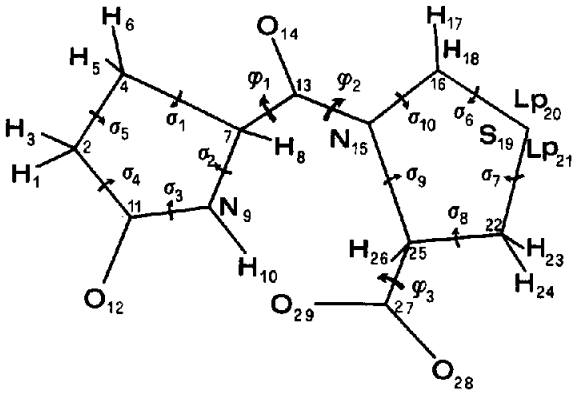

Fig. 1. Molecular structure of the conjugate base of PIDOTIMOD and definition of torsion angles.

structural fluctuations and the correlation coefficients of pairs of torsion angles were investigated.

We have taken into account the conjugate base of PIDOTIMOD since its pK_a is so low (3.03) that, under physiological conditions (pH $\approx$ 7), it is present almost completely in the ionized form; it can thus be hypothesized that the conjugate base is the bioactive form of the molecule.

The results of the calculations are compared with NMR spectra. Conformational calculations and NMR spectra identify two classes of conformers, trans and cis, around the peptide bond between the rings.

The hydrogen bonds in all the conformers have been investigated.

Experimental

Materials

PIDOTIMOD was synthesized in the laboratories of Poli Industria Chimica S.p.A. [1].

The pK_a of PIDOTIMOD was determined by potentiometric titration using an automatic titrator Mettler DL-25 with a glass electrode DG-111. The electrode was calibrated using buffer solutions at pH 4 and 7. A solution of 0.1 M KOH was used as a titrant and a solution of 0.49 mM potassium acid phthalate was used as a standard. A sample solution of 83 mM was used. pK_a was determined as the pH corresponding to 50% of the titrant volume at neutralization [4]. Ten measurements were performed and a pK_a of 3.03 ± 0.03 was obtained.

NMR measurements

^{1}H and ^{13}C NMR spectra were recorded on a Varian Gemini spectrometer operating at 200 MHz at a probe temperature of 21°C. Samples were prepared by dissolving about 50 mg of the compound in D_2O (1 ml) and correcting the pH at 7.0 with 1 M NaOD in D_2O.

Theoretical computations

The model force field

The AMBER program [5–8] was used for molecular mechanics and normal mode analysis calculations. The force field equation is of the form

$$U_{tot} = \sum_{bonds} k_r(r - r_{eq})^2 + \sum_{angles} k_\tau(\tau - \tau_{eq})^2 + \sum_{dihedrals} U_n/2[1 + \cos(n\phi - \delta)] + \sum_{i<j} w(A_{ij}/R_{ij}^{12} - B_{ij}/R_{ij}^{6} + 332.2q_iq_j/\epsilon R_{ij}) + \sum_{H-bonds} (C_{ij}/R_{ij}^{12} - D_{ij}/R_{ij}^{10})$$

The calculations were carried out on a VAX 8530 computer under the VMS 5.4 operating system. Throughout the calculations the all-atoms force field was used, i.e. all atoms were explicitly represented by the force field. The force field parameters were taken from ref. 5. An adequate description of a sulphur atom requires the explicit inclusion of lone pairs. The 1–4 non-bond and electrostatic interactions were weighted by a scale factor $w = 0.5$ and no cut-off for the non-bonded interactions was used. In the Coulomb term the value of the dielectric constant (relative

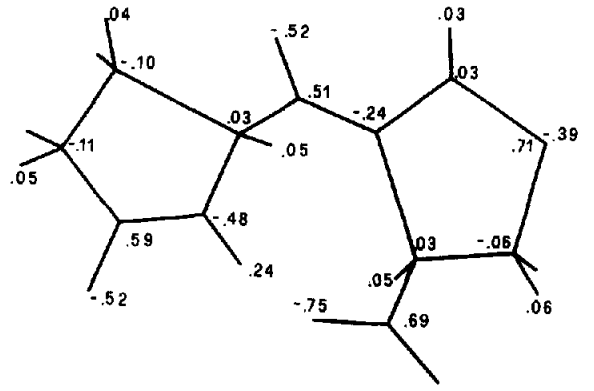

Fig. 2. Electrostatic potential derived net atomic charges.

permittivity) ϵ was taken as unity. Net atomic charges, q_k, were derived by fitting the quantum mechanically derived electrostatic potentials to a point charge model. Non-empirical electrostatic potentials [9] were computed with a density of 70 points nm^{-2} at the STO-3G basis set level with the GAUSSIAN 80 UCSF program [10,11] over four shells, with increments of 0.2 Å and starting from a scale factor of 1.4 of the van der Waals radii. The best fit of the electrostatic potentials was achieved using as an initial estimate the Mulliken charges, which were fully optimized with the Levenberg–Marquardt algorithm [12]. After optimization, the root-mean-square (r.m.s.) fit parameter is less than 0.01 kcal mol^{-1}. The results are reported in Fig. 2.

Energy minimization and vibrational analysis

In Fig. 1 the molecular structure of the conjugate base of PIDOTIMOD and the definition of the torsional angles are shown. We have applied a grid search procedure [13] to explore systematically the conformational subspace defined by the torsional angles outside the rings: ϕ_1 (C_4–C_7–C_{13}–N_{15}), ϕ_2 (C_7–C_{13}–N_{15}–C_{16}) and ϕ_3 (C_{22}–C_{25}–C_{27}–O_{28}) (Fig. 1). By varying ϕ_1 from 0 to 360°, ϕ_3 from 0 to 180° (because of the C_{2v} local symmetry on the $-COO^-$ group) with a grid spacing of 30°, and assuming for ϕ_2, values of 0 and 180° (at which the intrinsic torsional potential has a minimum), a set of 144 conformations was selected as a starting point for energy minimizations. The starting geometries were obtained with the program DIANA [14]. The cartesian coordinates obtained were used in the MINIM module of AMBER [5]. The powerful cartesian-coordinate energy minimization, in which the complete geometry optimization of all degrees of freedom is carried out, was used [15].

The energy minimization was carried out in two stages with modules of AMBER.

First, with the MINIM module, the steepest descent method was used for ten cycles; then the conjugate gradient was switched on, with a convergence criterion of 0.001 kcal mol^{-1} $Å^{-1}$ of r.m.s. energy gradient. This accuracy is necessary for the second stage. The conformations obtained in the first stage were selected by the following sorting procedure: they were ordered by increasing energy, and equivalent conformations were discriminated by checking the differences in the torsion angles ϕ_1, ϕ_2 and ϕ_3, with a tolerance of 15°; only if all torsions were "equal" were the conformations considered equivalent. Twelve non-equivalent conformations were determined and used in the subsequent stage.

Second, with the NMODE module, a quasi-Newton–Raphson method, using the analytically evaluated second derivatives of the energy, was used, with a convergence criterion of 10^{-8} kcal mol^{-1} $Å^{-1}$ of r.m.s. energy gradient. This accuracy is necessary for the subsequent normal mode analysis calculations. The mass-weighted second-derivative matrix of the potential energy at the minimum in cartesian space was computed. The vibrational frequencies and amplitudes of the normal mode were determined by diagonalizing the matrix [15]. By checking the six lowest frequency vibrations it was assured that each stationary point was a true minimum and not a maximum or a saddle point on the potential energy surface. Five non-equivalent conformers were determined.

From the normal mode frequencies ν_i, the harmonic vibrational contribution to the thermodynamic variables of state were calculated

using the established formulae [15–17]:

$$E = U + E_0 + E_T$$

$$E_0 \sum_i h\nu_i/2$$

$$E_T = \sum_i h\nu_i/(e^{h\nu_i/kT} - 1)$$

$$H = E + RT$$

$$-TS = \sum_i [kT\ln(1 - e^{-h\nu_i/kT}) - h\nu_i/(e^{h\nu_i/kT} - 1)]$$

$$G = H - TS$$

where U, E_0, E_T, E, H, S and G are the potential energy, vibrational zero-point energy, vibrational thermal energy, internal energy, enthalpy, entropy and Gibbs free energy, respectively, h is Planck's constant, T is the absolute temperature and k is Boltzmann's constant. All energies have been reported as differences with respect to the values of the conformer with the lowest potential energy. In all calculations T was taken as 298.15 K.

In order to roughly simulate the conformers in their media and adapt the conformational population from the theoretical calculations to give the experimentally determined ones in aqueous solution, the dielectric constant ϵ was taken as 5, 6, 7, 8, 9 and 10 and energy minimizations restarted from the conformers previously determined at $\epsilon = 1$. This, of course, does not take into account all the detailed effects induced by the solvent molecules due to their local interactions with the solute molecule. The NMODE module was used, with a convergence criterion of 10^{-8} kcal mol^{-1} Å^{-1} of r.m.s. energy gradient, and the eigenvalues of the second-derivative energy matrix were checked.

Normal mode dynamics

Normal mode dynamics [18] is a complementary method to the simulation of molecular dynamics trajectories and is particularly well suited to the study of slow processes, such as collective motions or conformational rearrangements. The motion can be described at each separate frequency or as a more complicated superposition of modes. The complete dynamics behaviour of the system is given by

$$Q_i = Q_{0i} + \sum_k A_{ik}\alpha_k \cos(\omega_k t + \delta_k)$$

with $\alpha_k = (2kT/\omega_k^2)^{1/2}$, $i = 1, \ldots, 3N$ and $k = 1, \ldots, 3N - 6$ where N is the number of atoms, Q_i are the atomic cartesian coordinates in the vicinity of the potential energy minimum at Q_{0i}, $A_{ik}\alpha_k$ are the amplitudes of the atoms, ω_k is the angular frequency and δ_k is the phase in the kth normal mode of the motion. Time-averaged properties, such as structural fluctuations and correlation coefficients of pairs of torsions, have been calculated from a data set of parameters as a function of time in normal mode dynamics. The motion of all atoms in a single normal mode is, by definition, completely correlated. The superposition of all modes reduces the extent of correlation; nevertheless, significant correlations can persist. The correlation coefficients C_{ij} for two torsions i and j can be estimated from a data set with the usual formula [19]:

$$C_{ij} = \sigma_{ij}/(\sigma_{ii}\sigma_{jj})^{1/2} = \sum[(x_i - \bar{x}_i)(x_j - \bar{x}_j)]/$$
$$\left\{\left[\sum(x_i - \bar{x}_i)^2\right]\left[\sum(x_j - \bar{x}_j)^2\right]\right\}^{1/2}$$

$C_{ij} = 1$ if torsions i and j move in the same direction for all modes (perfectly correlated), -1 if they move in opposite directions for all modes (perfectly anticorrelated), and 0 if there is no relationship between the motions in different modes (uncorrelated).

Results and discussion

NMR

The ^{1}H NMR spectrum of PIDOTIMOD recorded at pH $\approx$ 7 (D_2O) indicates an equilibrium mixture of the trans and cis conformers around the bridged peptide bond, with relative

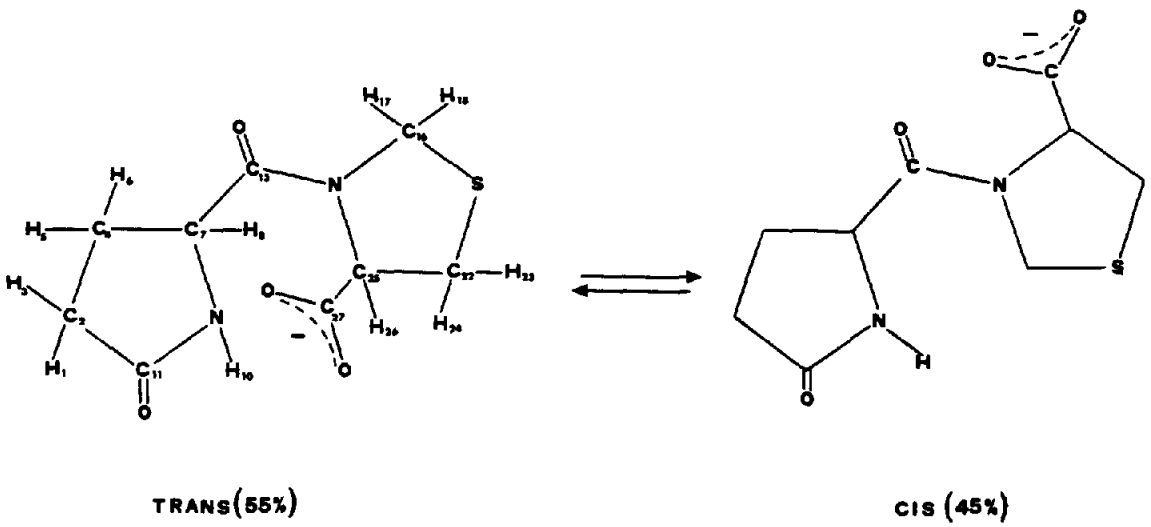

Fig. 3. Trans and cis conformers evidenced by NMR. Labels used to identify protons and carbon atoms are also shown.

conformational populations of 0.55 and 0.45, respectively (Fig. 3).

Assignments (see Table 1) were made on the basis of a COSY spectrum and confirmed by simulated spectra of the ABX system. The assignments are in agreement with those derived from previous investigations on similar compounds [20].

Qualitative experiments at different temperatures have shown that coalescence occurs near 75°C.

The ^{13}C NMR spectrum also corresponds to a mixture of two conformers. The assignments of the carbon chemical shifts have been made by comparison with the values found for pyroglutamic

Table 1
Assignments of signals of the ^{1}H NMR spectra

δ (ppm)[a]		
4.77 and 4.55	AB system $J_{AB} = -10$ Hz	H_{17} and H_{18} (trans)
4.60 and 4.55	AB system $J_{AB} = -11$ Hz	H_{17} and H_{18} (cis)
4.41	dd, $J = 5.0$, $J' = 9.0$	H_8 (trans)
4.75	dd, $J = 5.0$, $J' = 7.0$	H_8 (cis)
4.67	X part of ABX system $J_{XA} = 8.2$, $J_{XB} = 4.8$	H_{26} (trans)
4.66	X part of ABX system $J_{XA} = 6.4$, $J_{XB} = 3.6$	H_{26} (cis)
3.08 and 3.30	AB part of ABX system $J_{AB} = -12.8$, $J_{AX} = 8.2$, $J_{BX} = 4.8$	H_{23} and H_{24} (trans)
3.32 and 3.38	AB part of ABX system $J_{AB} = -12.0$, $J_{AX} = 6.4$, $J_{BX} = 3.6$	H_{23} and H_{24} (cis)
1.90–2.65	Multiplets	H_1, H_3, H_5, H_6, (cis and trans)

[a] TMS reference.

and thiazolidine-4-carboxylic acid at pH 7.0 (D_2O).

Theoretical calculations

The five conformers arrived at using the described procedure of minimization are listed in Table 2. Conformers are ordered with respect to their potential energy. The conformers lie within an energy range of 5 kcal mol^{-1}: trans conformers (A, B and C) are more stable than cis ones (D and E) by at least 0.7 kcal mol^{-1}. The higher stability of the trans conformers with respect to the cis is essentially due to the differences in their torsional, non-bonded and electrostatic energies.

The relative stability of the conformers, taking into account their free energy G, is significantly modified: the trans conformers A and B are clearly the most stable, followed by the cis conformer D, which is now more stable than the trans conformer C; the cis conformer E is the least stable. The zero-point vibrational energy E_0, the thermal vibrational energy E_T and the entropic term $-TS$ have an analogous trend, and indicate that the trans B and cis D conformers become more stable, and the trans C and cis E conformers become less stable.

Both the Boltzmann probabilities calculated from U and G, w_U and w_G respectively, indicate that the equilibrium conformational population is largely represented by the trans conformers.

The torsion angle ϕ_1 can assume three significantly different values: 160°, −70 to −100°, 80°. From the analysis of the models, values of $\phi_1 = 160°$ and $\phi_1 = -70$ to $-100°$ correspond to the oxo-prolyl ring being oriented as far as possible from the thiazolidine ring (exo-like arrangement). $\phi_1 = 180°$ corresponds to the oxo-prolyl ring being oriented as near as possible to the thiazolidine ring (endo-like arrangement).

The peptide torsion $|\phi_2|$ obviously assumes only two values, 180° and 0°, corresponding to trans (A, B and C) or cis (D and E) conformers, respectively.

The torsion angle ϕ_3 assumes three values: 60°, 110° and 40°. The first value corresponds to one of the carboxylic oxygen atoms eclipsed with respect to the peptide N_{15}. The second value corresponds to one of the carboxylic oxygen atoms eclipsed with respect to H_{26}, and to the absence of H-bonds. Lastly, the third value corresponds to the carboxyl group partially staggered and oriented orthogonally with respect to the bond C_{25}–H_{26}.

The H-bond O_{12}–H_{10} (C_4 type) is present in all the conformers and it is always weak (2.6 Å); the H-bond O_{14}–H_{10} (C_5 type) is present in the trans conformer B and in the cis D, being weaker in the former than in the latter (2.6 and 2.4 Å, respectively); the H-bond O_{29}–H_{10} (C_8 type) is present in the trans conformer C and in the cis E, always being strong (1.8 - 1.9 Å); the H-bonds O_{14}–H_{10} and O_{29}–H_{10} never coexist. There are three H-bond patterns: (1) O_{12}–H_{10}; (2) O_{12}–H_{10} and O_{14}–H_{10}; (3) O_{12}–H_{10} and O_{29}–H_{10}. The formation of the strong H-bond O_{29}–H_{10} occurs in the less stable trans and cis conformers, C and E, respectively.

In Fig. 4 the orthogonal projections with respect to the plane of the bridged peptide unit are reported for each conformer. In all conformers the oxo-prolyl ring has a pentane periplanar-like conformation [21], i.e. unless there are small deviations, all heavy atoms are coplanar; the thiazolidine ring has a pentane envelope-like conformation [21], i.e. one of the heavy atoms (C_{22} in A, C, D and E, S_{19} in B) is out of the plane defined by the other four. The two prochiral faces of the bridged peptide show steric hindrance which is typical for each conformer; similarly for the relative arrangement of the atomic groups.

The conformers obtained restarting the energy minimizations from the five conformers previously determined at $\epsilon = 1$ (Table 2 and Fig. 4), taking ϵ as 5, 6, 7, 8, 9 and 10, are reported in Table 3. The torsions ϕ_1 and ϕ_2 are invariant with respect to ϵ and practically equal to those obtained at $\epsilon = 1$. In contrast, the torsion ϕ_3 varies substantially

Table 2
Energy values (kcal mol^{-1}), normalized Boltzmann factors, torsion angles (deg) and H-bond (Å) patterns of H_{10} in all conformers

Conformer	U	w_u	U_{bond}	U_{angle}	U_{dihed}	U_{nb}	U_{al}	E_{hb}	G	w_G	E_0	E_T	$-TS$	ϕ_1	ϕ_2	ϕ_3	O_{12}	O_{14}	O_{29}
A	0.00	0.887	0.00	0.00	0.00	0.00	0.00	0.00	0.000	0.717	0.000	0.000	0.000	−158.78	178.08	54.93	2.609		
B	0.84	0.107	0.10	−0.39	0.59	−0.025	0.96	−0.40	0.557	0.280	−0.192	−0.056	−0.040	−101.60	−176.02	107.48	2.607	2.649	
C	3.11	0.005	0.10	2.27	0.038	0.24	0.59	−0.13	5.488	0.000	0.736	0.477	1.158	78.68	−177.20	37.30	2.661		1.817
D	3.79	0.001	−0.025	−0.67	1.63	0.080	2.57	0.20	3.431	0.002	−0.154	−0.061	−0.146	−67.04	4.781	63.09	2.631	2.404	
E	4.99	0.000	−0.013	0.060	5.02	0.40	−0.39	−0.090	6.324	0.000	0.402	0.302	0.631	−166.60	13.98	62.27	2.658		1.939

Table 3
Energy values (kcal mol^{-1}), normalized Boltzmann factors, torsion angles (deg) and H-bond (Å) patterns of H_{10} in all conformers as a function of the dielectric constant ϵ

	U	w_U	G	w_G	E_0	E_T	$-TS$	ϕ_1	ϕ_2	ϕ_3	O_{12}	O_{14}	O_{29}
$\epsilon = 5$													
A	0.000	0.576	0.000	0.592	0.000	0.000	0.000	−160.3	−178.4	82.9	2.6		
B	0.603	0.208	1.095	0.093	0.010	0.047	0.435	−102.9	−174.4	103.4	2.6	2.8	
C	2.103	0.016	2.926	0.004	0.133	0.050	0.640	75.0	−175.8	64.1	2.6		2.3
D	0.820	0.144	0.490	0.259	−0.124	−0.036	−0.170	−71.2	1.9	85.4	2.6	2.6	
E	1.387	0.055	1.444	0.052	0.024	0.067	−0.034	−161.8	2.1	84.8	2.6		
$\epsilon = 6$													
A	0.000	0.543	0.000	0.525	0.000	0.000	0.000	−160.4	−178.1	85.7	2.6		
B	0.637	0.185	1.125	0.079	0.012	0.048	0.428	−103.0	−174.3	103.3	2.6	2.8	
C	1.984	0.019	2.673	0.006	0.102	0.034	0.553	74.6	−175.6	67.9	2.6		2.4
D	0.660	0.178	0.294	0.320	−0.128	−0.038	−0.200	−71.2	1.8	88.0	2.6	2.6	
E	1.171	0.075	1.192	0.070	0.018	0.063	−0.059	−161.7	1.9	87.2	2.6		
$\epsilon = 7$													
A	0.000	0.513	0.000	0.468	0.000	0.000	0.000	−159.8	−178.0	85.9	2.6		
B	0.665	0.167	1.138	0.068	0.012	0.048	0.414	−103.0	−174.3	103.1	2.6	2.8	
C	1.888	0.021	2.484	0.007	0.083	0.024	0.490	74.3	−175.5	70.9	2.6		2.5
D	0.543	0.205	0.140	0.370	0.132	−0.040	−0.231	−71.2	1.7	90.0	2.6	2.6	
E	1.015	0.093	0.998	0.087	0.012	0.059	−0.088	−161.7	1.8	89.2	2.6		
$\epsilon = 8$													
A	0.000	0.488	0.000	0.421	0.000	0.000	0.000	−160.5	−177.8	88.8	2.6		
B	0.687	0.153	1.146	0.061	0.011	0.049	0.400	−103.1	−174.3	103.0	2.6	2.8	
C	1.808	0.023	2.350	0.008	0.071	0.018	0.453	74.1	−175.4	73.3	2.6		2.5
D	0.453	0.227	0.018	0.409	−0.135	−0.040	−0.259	−71.2	1.6	91.7	2.6	2.6	
E	0.896	0.108	0.846	0.101	0.008	0.057	−0.114	−161.6	1.7	90.8	2.6		
$\epsilon = 9$													
A	0.000	0.467	0.000	0.384	0.000	0.000	0.000	−160.5	−177.7	89.7	2.6		
B	0.705	0.142	1.150	0.055	0.010	0.048	0.387	−103.1	−174.2	102.9	2.6	2.8	
C	1.742	0.025	2.252	0.009	0.063	0.013	0.433	73.9	−175.2	75.0	2.6		2.5
D	0.381	0.245	−0.080	0.440	−0.138	−0.041	−0.283	−71.2	1.5	93.1	2.6	2.6	
E	0.801	0.121	0.725	0.113	0.004	0.055	−0.136	−161.6	1.6	92.1	2.6		
$\epsilon = 10$													
A	0.000	0.449	0.000	0.353	0.000	0.000	0.000	−160.5	−177.6	90.4	2.6		
B	0.720	0.133	1.154	0.050	0.010	0.048	0.376	−103.1	−174.2	102.9	2.6	2.9	
C	1.687	0.026	2.180	0.009	0.058	0.011	0.423	73.8	−175.2	76.4	2.6		2.6
D	0.323	0.260	−0.161	0.464	−0.140	−0.042	−0.303	−71.2	1.5	94.3	2.6	2.6	
E	0.725	0.132	0.626	0.123	0.002	0.054	−0.155	−161.6	1.6	93.3	2.6		

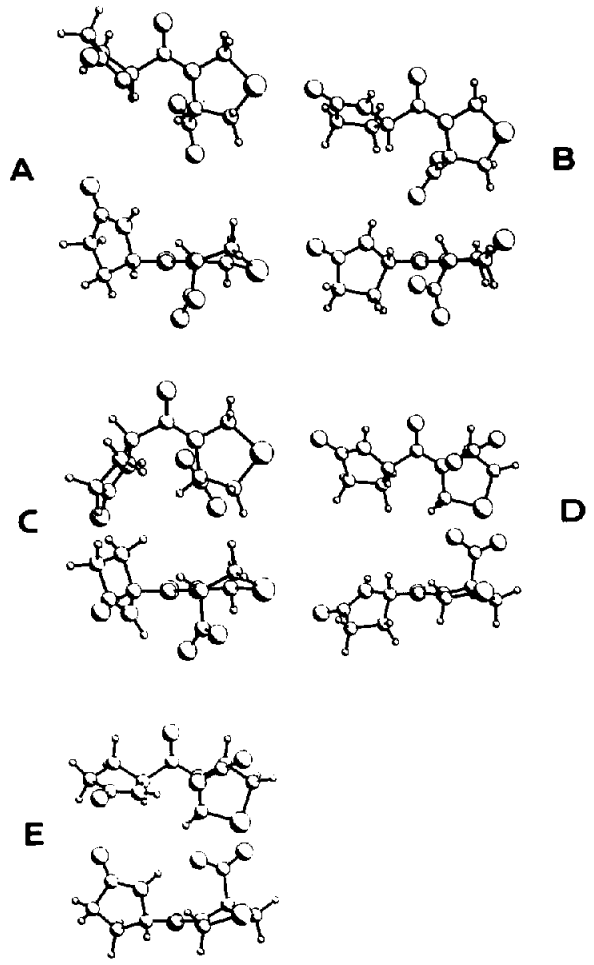

Fig. 4. Orthogonal projections with respect to the plane of the bridged peptide unit for all conformers, obtained from the minimization procedure.

on passing from $\epsilon = 1$ to $\epsilon = 5$ (up to 40°) and to a lesser extent for $5 \leq \epsilon \leq 10$ (up to 12°).

The H-bond pattern of the cis conformer E is modified with the loss of the bond with the carboxyl group $-COO^-$ for $\epsilon \geq 5$. In general, as expected, the H-bonds become gradually weaker (in particular, those involving $-COO^-$) as ϵ increases.

We shall now analyze the trend of the values of the parameters as a function of ϵ. By taking into account the potential energy U (or the Boltzmann probabilities w_U), the trans conformers A and C are the most and the least stable, respectively, for all ϵ values. The relative stability of the cis conformers increases on increasing the ϵ values. By taking into account the free energy G (or the Boltzmann probabilities w_G), the trans A and cis D conformers are found to be the most stable at $\epsilon \leq 8$ and at $\epsilon \geq 9$, respectively. The cis conformer D has the lowest zero-point and thermal vibrational energies, E_0 and E_T, at all ϵ values; the energy differences of E_0 between the conformers are more or less constant as a function of ϵ, and those of E_T vary a little. By considering the entropic contribution, the cis conformers appear to be the most stable with considerable differences which increase on increasing ϵ. Then for $\epsilon \geq 5$, both trans and cis conformers are represented to a significant extent.

At $\epsilon = 7$ the trans and cis Boltzmann probabilities ($w_G^{trans} = 0.54$ and $w_G^{cis} = 0.46$) agree perfectly with the experimentally determined conformational populations.

In Fig. 5 the motions of the atoms (except hydrogen atoms which cannot form H-bonds) in the lowest ten frequency modes (from 27 to 258 cm^{-1}) for conformer A are taken into account in three-dimensional models. Only the lowest modes such as those whose r.m.s. torsion fluctuation is just greater than or equal to 70% of the r.m.s. due to all the modes are taken into account. The motions are collective in that they involve a simultaneous shift of all atoms (or rotation of all atomic groups) of the molecule. We will analyze larger atomic motions and rotational librations of atomic groups around torsion angles. The extent of the latter is expressed as r.m.s. fluctuations, which have been calculated from normal mode dynamics of each separate frequency and are reported in Table 4. The shift arrows of the prolyl atoms in mode I are in the plane of the ring and the group librates with a rigid body-like motion around the torsion angle ϕ_1; in the other modes the oxo-prolyl atoms move from up to down the plane of the ring. The bridged carbonyl group moves out-of-plane in all modes. The extent of the motions of the thiazolidine atoms are generally small, and C_{16}, C_{22} and S_{19} move out-of-plane of the ring. The shift arrows on the

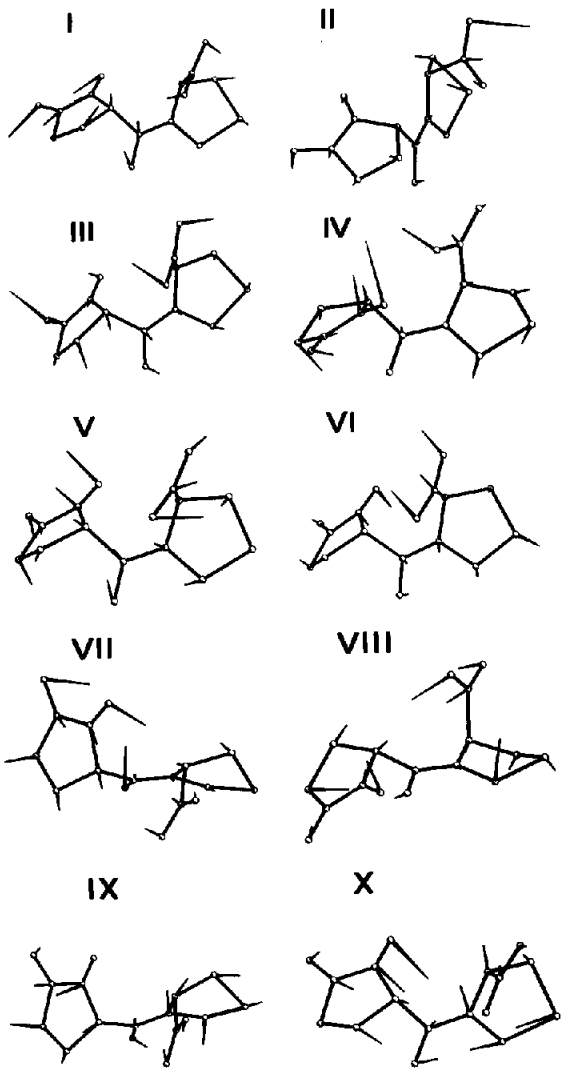

Fig. 5. Motions of the atoms in the lowest ten frequency normal modes for conformer A in three-dimensional models. Hydrogen atoms which cannot form H-bonds are not reported.

carboxyl oxygen atoms point out-of-plane in modes from I to VIII with large twisting motions and the group moves as a rigid body around the torsion ϕ_3; in modes IX and X the oxygen atoms move in-plane with a rocking motion. The extent of the torsional fluctuations in the rings, σ_i, is small for all modes.

In Table 4 the r.m.s. torsional and H-bond distance fluctuations for each conformer derived from normal mode dynamics, in which the superposition of all modes is considered, is shown. The extent of ϕ_3 fluctuation around the carboxyl group is in the range from 11.6 to 15.3° and is the largest in all the conformers; the trend, analogous to that of the calculated free energy, indicates the important role that this libration plays. ϕ_1 fluctuation is the second in amplitude (except for the cis conformer E) and is particularly large in the most stable conformer A. The extent of fluctuation of ϕ_2 around the peptidic bond between the two rings varies from 8.3 to 9.5° and it is larger for the cis than for the trans conformers.

Table 4
R.m.s. torsional and H-bond distance fluctuations for all conformers by normal mode dynamics

	Conformers				
	A	B	C	D	E
Torsions					
ϕ_1	14.96	9.69	9.47	11.10	9.22
ϕ_2	8.27	8.51	8.19	9.48	8.88
ϕ_3	15.27	13.51	12.16	12.79	11.57
σ_1	6.43	9.69	6.88	8.51	7.12
σ_2	6.66	8.85	6.82	8.10	7.29
σ_3	7.01	7.23	6.89	7.30	6.88
σ_4	6.98	7.74	7.17	7.47	6.78
σ_5	6.49	9.04	6.91	8.06	6.77
σ_6	6.79	5.90	7.39	7.42	8.67
σ_7	5.12	5.54	5.33	5.39	6.45
σ_8	5.55	7.37	4.63	5.31	5.27
σ_9	7.85	8.83	7.02	7.85	7.63
σ_{10}	8.61	8.07	8.75	9.11	9.90
H-bonds					
O_{12}	0.086	0.088	0.080	0.088	0.082
O_{14}		0.232		0.197	
O_{29}			0.113		0.233

The molecular mobility of the conformers is strongly determined by their H-bonds. Conformers characterized by the same H-bond pattern have similar mobility. In Fig. 6 the behaviour of the torsion ϕ_i and of the interaction distance O_{14}–H_{10} as a function of time in normal mode dynamics is reported for conformer A. The monitored geometric parameters fluctuate in different ways and to varying extents around their equilibrium value (harmonic approximation). ϕ_1 and ϕ_3 have

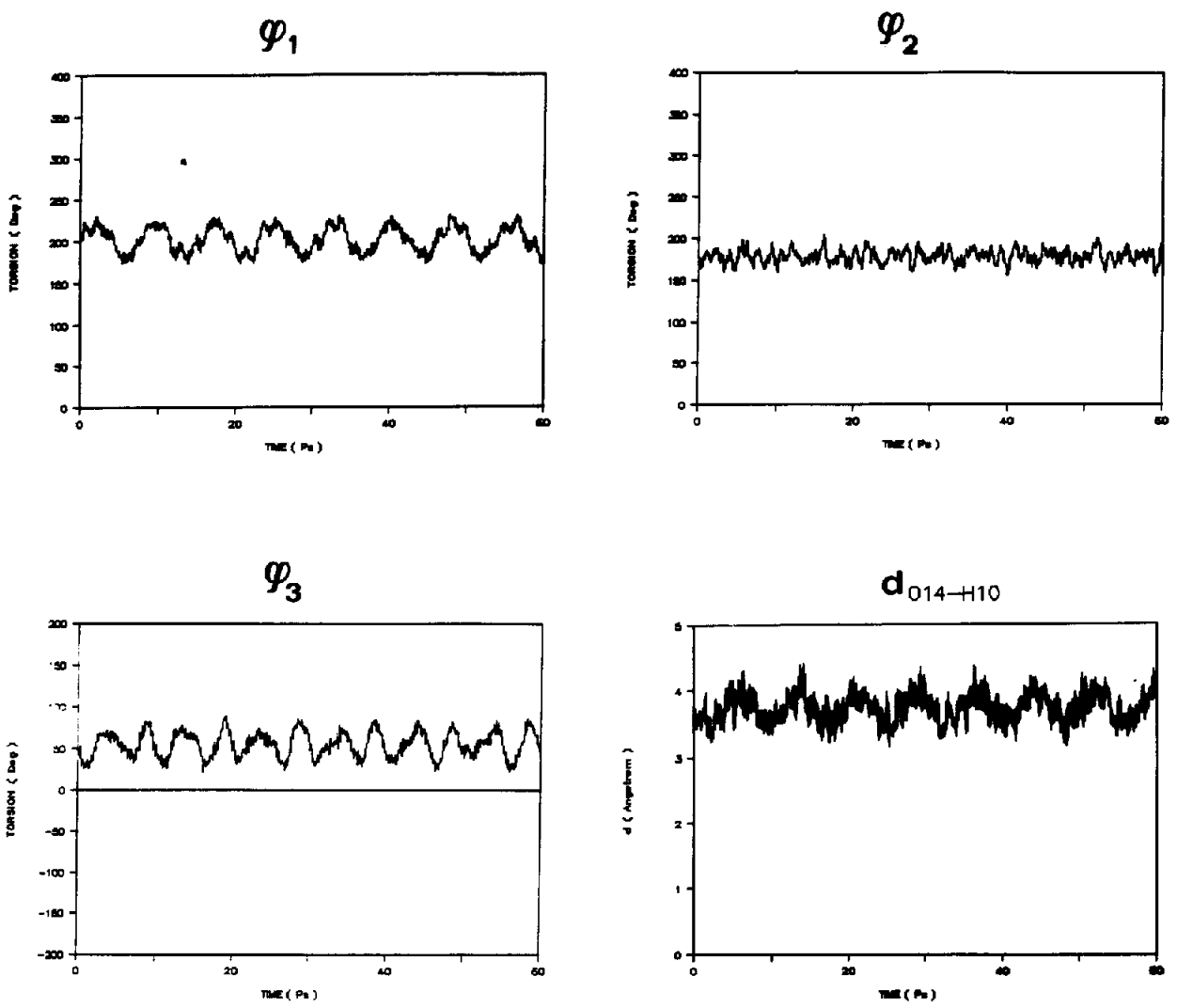

Fig. 6. Behaviour of ϕ_1, ϕ_2 and ϕ_3 torsions and $O_{14}-H_{10}$ interaction distance as a function of time in normal mode dynamics for conformer A.

a quasi-periodic behaviour as their dynamics are strongly characterized by the presence of a normal mode (the first and the second, respectively (Table 5)), whose extent of fluctuation is larger by at least one order of magnitude than that of the other modes, which are responsible for the observed dynamic noise. ϕ_2 has an aperiodic dynamic behaviour, as there are a number of normal modes whose extent of fluctuation is of the same order of magnitude (Table 5). The interaction distance $O_{14}-H_{10}$ has a quasi-periodic behaviour strictly related to the dynamics of the torsion ϕ_1.

Figure 7 shows the triangular map of the correlation coefficients, C_{ij}, of all pairs of torsions ϕ and σ from normal mode dynamics

Table 5
R.m.s. torsional fluctuations for the lowest ten frequency modes for conformer A

	Normal modes									
	1	2	3	4	5	6	7	8	9	10
ϕ_1	13.92	1.34	1.73	1.73	2.64	2.56	1.26	0.66	1.12	0.17
ϕ_2	0.88	3.19	3.11	0.91	2.85	2.81	1.66	3.23	2.57	1.07
ϕ_3	2.98	13.20	6.22	1.28	2.03	0.60	1.19	0.44	0.91	0.61
σ_1	1.55	0.65	1.37	2.27	1.83	1.35	2.23	2.51	1.64	1.66
σ_2	1.09	1.24	2.86	2.47	2.25	1.39	0.72	1.62	0.08	1.91
σ_3	0.12	1.32	3.16	1.60	1.72	0.83	3.46	0.05	1.63	1.39
σ_4	0.93	0.81	2.08	0.04	0.43	0.10	4.68	1.65	2.56	0.20
σ_5	1.50	0.04	0.32	1.35	0.90	0.87	4.01	2.41	2.38	1.02
σ_6	0.77	1.55	0.18	2.79	1.14	2.02	0.59	3.57	2.93	1.11
σ_7	0.44	0.11	1.08	0.73	0.07	2.67	0.65	2.09	2.12	0.39
σ_8	0.06	1.69	1.72	1.71	1.23	2.91	0.59	0.06	0.64	0.20
σ_9	0.59	3.05	1.69	4.03	2.22	1.62	0.19	2.72	1.50	1.05
σ_{10}	0.89	2.95	0.88	4.39	2.13	0.50	0.31	4.18	3.00	1.41

for all conformers. The C_{ij} values are multiplied by a factor of ten. From the analysis of Fig. 7 the following general features are deduced.

(1) The motion around ϕ_1 is always highly uncorrelated, except with ϕ_2 in conformer E (anticorrelated).

(2) For the trans conformers, ϕ_2 is anti-correlated and correlated with the next-neighbour torsions σ_9 and σ_{10}, respectively; for the cis conformers ϕ_2 is highly uncorrelated; in conformer B an interesting correlation with the second neighbour torsion σ_8 takes place.

(3) The torsions ϕ_3, ϕ_3' referring to O_{28} and ϕ_3'' to O_{29}, are perfectly correlated (rigid body-like motion of the carboxyl group).

(4) The librational motions around σ_1, $\sigma_2, \ldots, \sigma_{10}$ are anticorrelated with the next-neighbour σ torsions (for example, σ_1 with σ_2 and σ_5, σ_{10} with σ_6 and σ_9).

(5) A number of correlations among the second-neighbour σ torsions takes place, in particular the motion around σ_1 is correlated with σ_4 except in conformer A; σ_2 in conformers D, B and E is correlated with σ_5; σ_6 is always correlated with σ_9; σ_7 is correlated with σ_{10} except in conformer B in which σ_{10} is correlated with σ_8. We observe that σ_3 is always uncorrelated.

Conclusions

The conjugate base of PIDOTIMOD in aqueous solution, according to the NMR spectra, appears to be an equilibrium mixture of trans and cis conformers around the bridged peptide group, with relative conformational populations of 0.55 and 0.45, respectively. The conformational population from theoretical calculations is perfectly adapted to give the experimentally determined one by varying the value of the dielectric constant, the best agreement being obtained at $\epsilon = 7$. The conformational features show that the path connecting the trans and cis forms may involve the bridged peptide bond alone.

Three different H-bond patterns are determined: $O_{12} \cdots HN<$, $O_{12} \cdots HN<$ and $O_{14} \cdots HN<$, $O_{12} \cdots HN<$ and $O_{29} \cdots HN<$.

As regards the dynamic behaviour, the extent of the ϕ_1 and ϕ_3 torsional fluctuations is the largest in all the conformers. Their dynamic behaviour is strongly characterized (quasi-periodic motion) by the presence of one normal mode, which predominates over the others. The conformers' molecular mobility is strongly determined by their H-bonds. Conformers characterized by the same H-bond pattern have similar mobility.

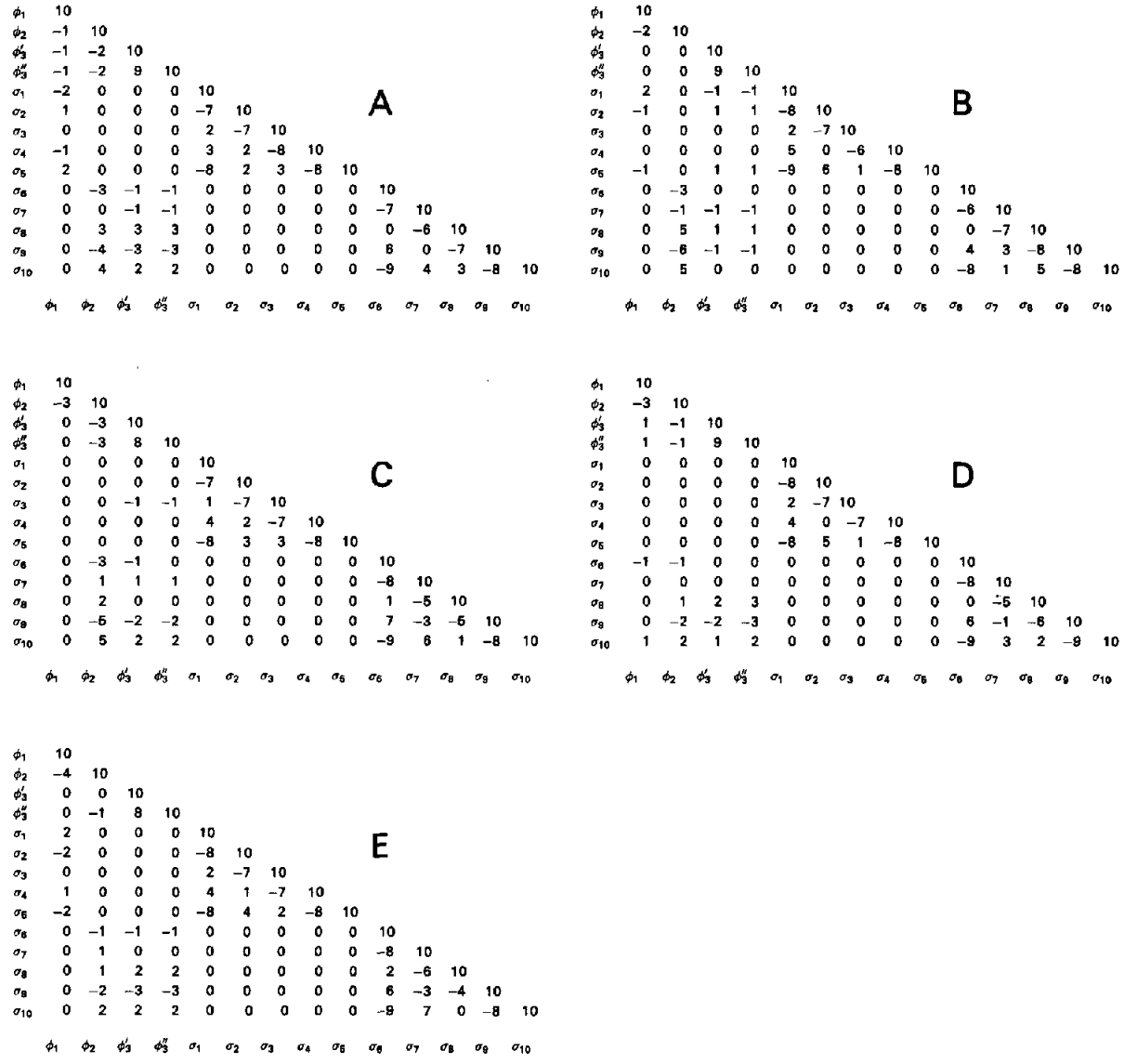

Fig. 7. Triangular maps of the correlation coefficients of all pairs of torsions ϕ_i and σ_i by normal mode dynamics for all conformers. The values are multiplied by a factor of ten.

Significant correlations hold in the motion of torsion angles.

The conformational features and the dynamic behaviour of the isolated molecule of PIDOTIMOD may be a useful starting point for gaining an insight into the molecular affinities between PIDOTIMOD and the IL-2 T-lymphocyte receptor. In order to study these dynamically stable structures and conformational transitions, molecular dynamics simulations are now in progress.

Acknowledgements

We would like to thank the CISIT of the Universita' della Basilicata. This work has been

partially supported by a grant from the Ministero della Universita' e della Ricerca Scientifica e Tecnologica (Italy).

References

1 S. Poli, U.S. Patent 4, 839, 387.
2 A. Auteri, A.L. Pasqui, F. Bruni, M. Saletti, M. Di Renzo and M. Tafani, 5th Int. Conf. on Immunopharmacology, Annecy, France, 15–17 May 1991.
3 G. Coppi and F. Mailland, Pharmacol. Res., 22 (1990) 126.
4 A. Albert and E.P. Serjeant, The Determination of Ionization Constants, T. and A. Constable, Edinburgh, 1971.
5 U.C. Singh, P.K. Weiner, J. Caldwell and P.A. Kollman, AMBER 3.0, University of California, San Francisco, CA, 1987.
6 S.J. Weiner, P.A. Kollman, D.T. Nguyen and D.A. Case, J. Comput. Chem., 7 (1986) 230.
7 P.K. Weiner and P.A. Kollman, J. Comput. Chem., 2 (1981) 287.
8 S.J. Weiner, P.A. Kollmann, D.A. Case, U.C. Singh, C. Ghio, G. Alagona, S. Profeta, Jr., and P. Weiner, J. Am. Chem. Soc., 106 (1984) 765.
9 E. Scrocco and J. Tomasi, J. Adv. Quantum Chem., 11 (1978) 115.
10 U.C. Singh and P.A. Kollman, GAUSSIAN 80 UCSF, QCPE Bull., 2 (1982) 17.
11 W.J. Hehre, R.F. Stewart and J.A. Pople, J. Chem. Phys., 51 (1969) 2657.
12 R. Fletcher, Practical Methods of Optimization, Wiley, New York, 1980.
13 H.A. Sheraga, Chem. Rev., 71 (1971) 195.
14 R. Fusco, DIANA, Internal Report, Istituto Guido Donegani, Novara, Italy, 1985.
15 S. Lifson and A.J. Warshel, J. Chem. Phys., 49 (1968) 5116.
16 F.L. Hill, An Introduction to Statistical Thermodynamics, Addison-Wesley, Reading, MA, 1960.
17 A.T. Hagler, P.S. Stern, R. Sharon, J.M. Becker and F. Naider, J. Am. Chem. Soc., 101 (1979) 6842.
18 M. Levitt, C. Sander and P.S. Stern, J. Mol. Biol., 181 (1985) 423.
19 I.F. Blake, An Introduction to Applied Probability, Wiley, New York, 1979.
20 F.A.M. Borremans, Bull. Soc. Chim. Belg., 89 (1980) 2.
21 J.B. Hendrickson, J. Am. Chem. Soc., 83 (1961) 4537.